# 1.D Beam Smoothing by Spectral Dispersion (SSD)

Techniques for improving laser beam uniformity currently involve breaking up the beam into a large number of beamlets whose diffraction-limited size is roughly the same as the target diameter. The resultant intensity pattern on target will be a smooth envelope superimposed upon a rapidly varying interference pattern from the overlap of the different beamlets. In the approach proposed by Kato[1] it is assumed that much of the interference structure would be eliminated by thermal smoothing within the target or by refraction of the beamlets in the target atmosphere. It is unlikely, however, that the very-long-wavelength structure will be eliminated. To eliminate nearly all the interference structure, a group at the Naval Research Laboratory has proposed the scheme of induced spatial interference (ISI)[2–4] whereby each beamlet is delayed by one or more coherence times so that the interference pattern on target fluctuates in time, resulting in a smooth time-averaged intensity profile. This technique requires a spectrally broad laser pulse (i.e., a short coherence time) to achieve smoothing in a time smaller than the characteristic hydrodynamic time scale of the target. However, due to the narrow spectral bandwidth required to achieve high-efficiency frequency tripling, the application of ISI has to date been ruled out for a frequency-tripled system such as OMEGA or NOVA. Two alternative approaches[5,6] also require a spectrally broad laser pulse.

We are proposing a new technique to smooth the interference pattern and still permit frequency tripling (or quadrupling). Like ISI, a broad bandwidth is required, but the spectrum is now dispersed spatially. Smoothing of the interference pattern is now achieved by the rapid temporal oscillations that result from the interference of the beamlets of different frequency. This smoothing may be faster than the superposition of the random intensity patterns achieved in ISI. Further, if the laser pulse can be spatially coded with a linear spectral variation, it is possible to achieve high-frequency tripling performance by simply compensating for the spectral variation with a linearly varying angle of incidence on the frequency converter. The spectral encoding can be accomplished, for example, by the use of dispersive optics such as gratings, while the angle-of-incidence variation can be achieved by the imposition of cylindrical divergence or convergence on the beam.

A possible use of this approach to reduce the modulation produced by the interference of distributed phase plate (DPP) beamlets on target is shown schematically in Fig. 36.13. A broadband pulse, produced either by a broadband oscillator or by propagation of a narrow-bandwidth pulse through a fiber or a suitable nonlinear medium, is dispersed spectrally with a pair of gratings producing a beam of approximately rectangular cross section with linear variation in wavelength along the long direction. After correction of the beam shape with appropriate cylinder optics and apodizing aperture, the beam is propagated through the normal amplifier system. Prior to frequency conversion a weak cylindrical lens imposes a matched convergence to the beam, which is corrected with a negative lens

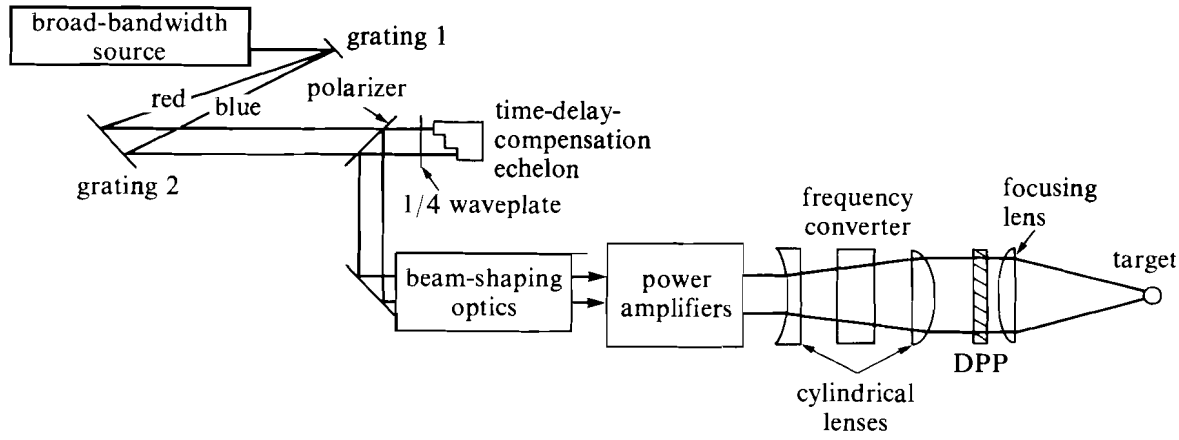


Fig. 36.13
Schematic of beam-smoothing system using spectral dispersion.

following the frequency converter. As an example, to compensate for a 10-Å variation in wavelength in one direction, a convergence (or divergence) of 1.6 mrad is required. The existing DPP's are used in conjunction with the spectrally broadened pulse to achieve nearly modulation-free beam envelopes for times much longer than the pulse mutual coherence time.

Computer code simulations of the interference pattern generated by the DPP's show that for times larger than 25 - 50 coherence times the beam pattern on target is nearly modulation free. This is the result of a spectral variation along only one direction (chosen to match the crystal cut ). If we require this smoothing time to be of order 25 ps to 50 ps, a bandwidth of approximately $10^{12}$ Hz is required at 0.35 $\mu$m, which corresponds to 10 Å at 1.054 $\mu$m (frequency tripling increases the pulse bandwidth by a factor of 3 in frequency). Since the gain bandwidth of the most commonly used laser glass, LHG-8, is 218 Å (FWHM), the energy capability of the high-power glass laser should not be reduced substantially by the increased bandwidth.

**Broad-Bandwidth Generation**

There are a number of alternative ways to generate a laser pulse with broad spectral bandwidth. The conventional ISI technique typically makes use of a $Q$-switched oscillator with appropriate intracavity etalons to generate the desired spectral content. The typical bandwidth generated by such oscillators is 100 Å or less. These oscillators produce pulses several tens of nanoseconds long and must therefore be further shortened by a pulse-chopping system.[2,6]

An alternative approach is to create the spectral broadening external to the oscillator. Through a combination of self-focusing and self-phase

modulation it is possible to obtain large spectral broadening and chirping by propagating an intense pulse through an optical fiber.[7] The degree of broadening and chirping is a function of the pulse energy, the pulse width, and the fiber length. This technique for bandwidth generation has the disadvantage of requiring a high degree of control on the input pulse parameters and is relatively inflexible.

Spectral broadening has been demonstrated by the use of an electro-optic phase modulator[8]; spectral bandwidths up to 600 GHz were demonstrated with a $LiTaO_3$ modulator driven by a 9.35-GHz, pulsed-microwave generator. This appears to be a promising way to broaden the spectral content of bandwidth-limited laser pulses.

**Spectral Dispersion**

Gratings offer the best technique for achieving the required levels of spectral dispersion. Using a linear grating where the first order diffracts close to retroreflection,[9] high reflectivity may be achieved.

Consider a beam incident on a grating with line spacing $d$ at an angle $\theta_i$ to the plane of the grating (Fig. 36.14). The grating equation relates the diffraction angle $\theta_r$ and the wavelength $\lambda$ by

$$\lambda = d[\cos\theta_i + \cos\theta_r(\lambda)] \ .$$

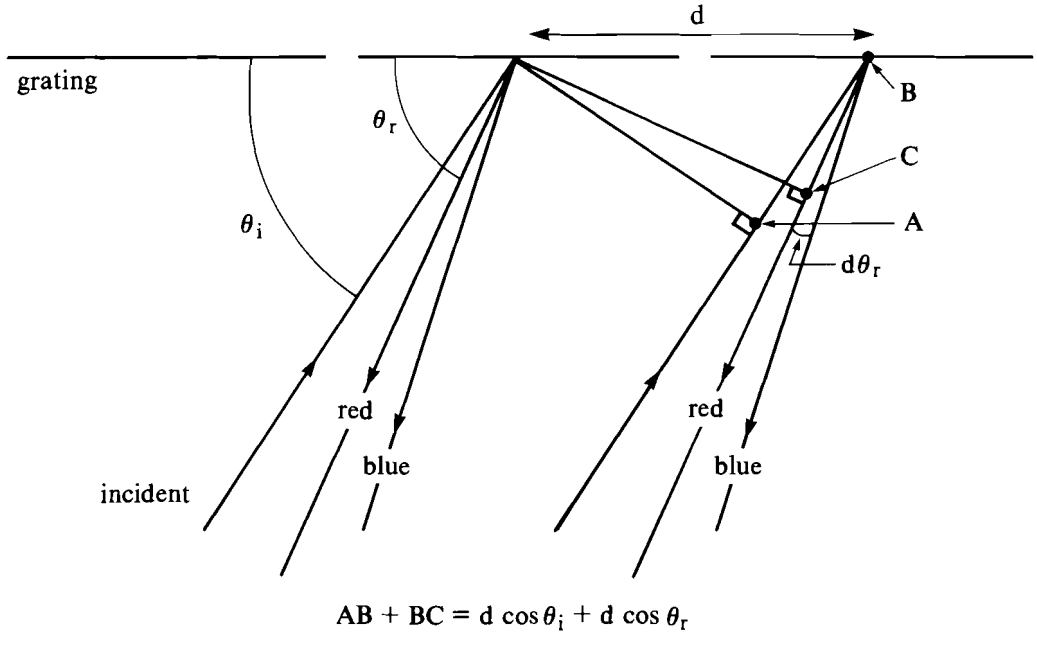


Fig. 36.14
Diffraction grating operated in first order close to retroreflection. The optical path difference between the red rays is shown as $AB + BC$. The blue rays emerge closer to the grating normal.

If $\lambda = \lambda_o + \Delta\lambda$ where $\lambda_o = 2d\cos\theta_o$, $\theta_o$ being the retro-angle for the central wavelength $\lambda_o$, then

$$\cos\theta_r(\lambda) = \frac{\lambda(2\cos\theta_o)}{\lambda_o} - \cos\theta_i \quad .$$

Differentiating, we obtain $\sin\theta_r \frac{d\theta_r}{d\lambda} = \frac{2\cos\theta_o}{\lambda_o}$ ,

so that

$$d\theta_r = -a\frac{d\lambda}{\lambda_o} \quad , \tag{1}$$

where $a \equiv 2\cos\theta_o/\sin\theta_r$. For typical conditions ($d = 0.588$ $\mu$m, $\lambda_o = 1.054$ $\mu$m, $\theta_r \approx \theta_o = 26.38°$), we have $a = 4.033$. If $\Delta\lambda = 10$ Å, $d\theta_r \simeq 4 \times 10^{-3}$ rad. Prisms would be unsuitable as they give dispersions about two orders of magnitude smaller.

To obtain efficient frequency tripling with this approach, we must have relatively high spectral dispersion so that the bandwidth of the dispersed beam at any one point $\lesssim 1$ Å. We can estimate the requirements on beam size $D$ and grating separation $L$, using the construction shown in Fig. 36.15.

If the source spectrum contains wavelengths from $\lambda_o$ to $\lambda_o + d\lambda_{max}$, and the resulting dispersion spreads the spectrum in the plane of the second grating over a length $y_{max}$, then

$$y_{max} \simeq Ld\theta_r \quad , \tag{2}$$

it being assumed that we are operating close to retroreflection, and

$$\lambda(y) = \lambda_o + (y/y_{max})\, d\lambda_{max} \quad .$$

At a point $y$, we see all wavelengths between $\lambda(y + D/2)$ and $\lambda(y - D/2)$, i.e., between

$$\lambda_o + \frac{y}{y_{max}} d\lambda_{max} \pm \frac{D}{2y_{max}} d\lambda_{max}$$

or

$$\lambda(y) \pm \frac{\delta\lambda}{2}$$

where

$$\delta\lambda = \frac{D}{y_{max}} d\lambda_{max} \quad . \tag{3}$$

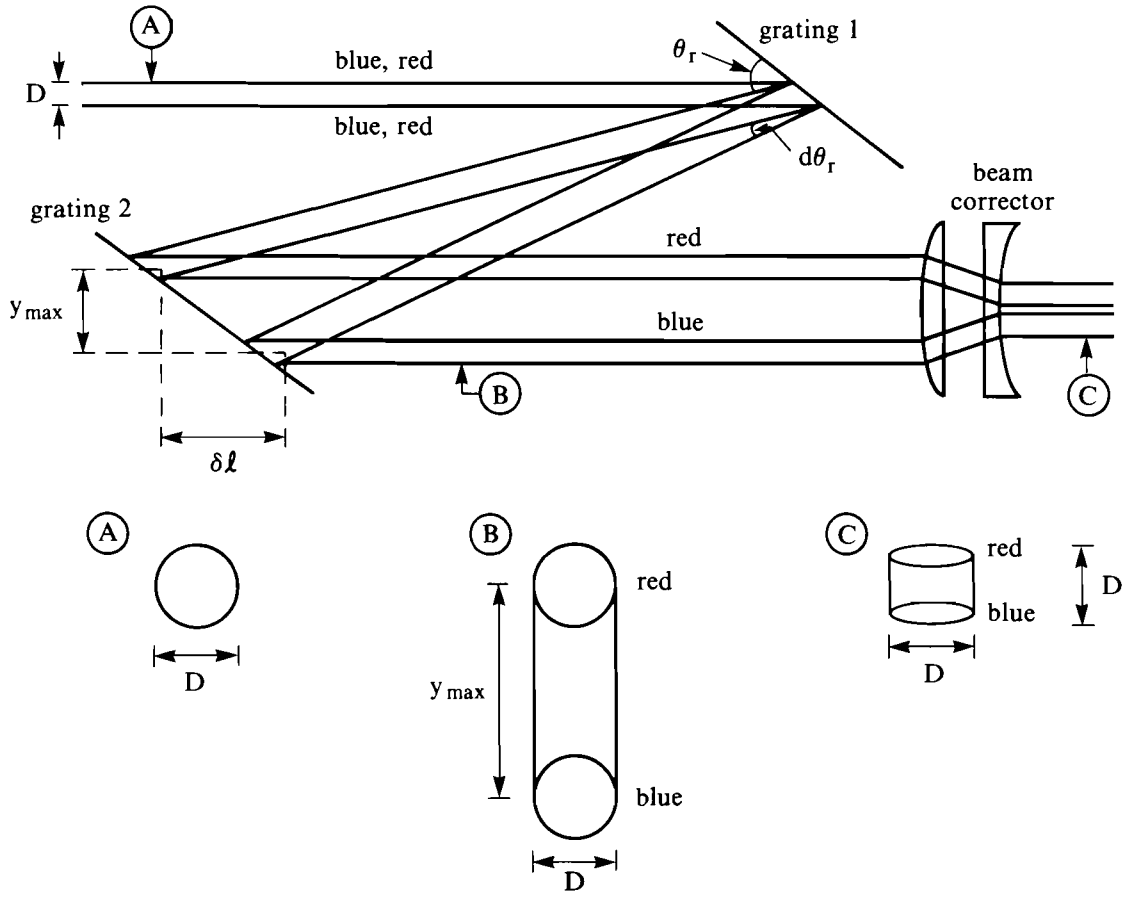


Fig. 36.15
Schematic showing change of beam shape while passing through a grating pair followed by a cylindrical collimator used to correct the beam shape. The time delay of the red component relative to the blue is approximately 2 $\delta\ell$.

Thus, the bandwidth is reduced after dispersion by the factor $y_{max}/D$, known hereafter as the spatial dispersion factor, the same factor by which the beam cross-section is elongated. For example, if $d\lambda_{max}$ = 10 Å, $\delta\lambda$ = 1 Å, and $D$ = 0.3 cm, then $y_{max}$ = 3 cm. Note that the grating separation required is determined by $\delta\lambda$ and not $d\lambda_{max}$ since [from Eqs. (1)-(3)]

$$\frac{D}{L} = a\,\frac{\delta\lambda}{\lambda_o} \quad .$$

In our case, with the requirement that $\delta\lambda/\lambda_o < 10^{-4}$ for high-frequency tripling, $D/L < 4 \times 10^{-4}$ regardless of $d\lambda_{max}$. For example, with $D$ = 0.3 cm, we require $L > 7.5$ m.

**The Effect of Diffraction**

The beam diameter $D$ spreads laterally with characteristic half-angle $\phi$ given by $\phi \sim \lambda_0/D$, and must be chosen to be sufficiently large that the added bandwidth is less than $\delta\lambda$.

After propagation through a distance $L$, the beam half-width increases by $\sim L\phi$. In order to avoid added bandwidth at distance $L$ we require $L\phi < D$, i.e., $L\lambda_0 < D^2$,

or

$$\frac{D}{\lambda_0} > \frac{L}{D} = \frac{1}{a}\frac{\lambda_0}{\delta\lambda}$$

or

$$D > \lambda_0 \left(\frac{1}{a}\frac{\lambda_0}{\delta\lambda}\right).$$

For $\delta\lambda/\lambda \lesssim 10^{-4}$ and $a \approx 4$, $D > 0.25$ cm, so that the assumed $D = 0.3$ cm is just large enough and we may have to increase $D$ to say 0.5 cm to assure high spectral purity.

**Beam Temporal Spread**

As may be evident from Fig. 36.15 the double-grating spectral disperser introduces a time delay across the beam that is linearly proportional to the imposed bandwidth. The red edge of the beam is delayed relative to the blue edge by a distance given approximately by

$$2\,\delta\ell = 2\,y_{max}\cot\theta_0 \approx a\,y_{max}\ ,$$

which, in our example ($y_{max} = 3$ cm), is 12 cm or 400 ps. Since DPP's are to be used for phase conversion in the proposed smoothing technique, this temporal delay eventually results in an effective temporal broadening of the pulse. One method of correcting for this delay is to employ appropriately designed echelons at the output of the grating disperser as shown in Fig 36.13.

**Frequency-Conversion Requirements**

Table 36.II summarizes the requirements imposed on beam alignment and wavelength when performing frequency tripling using two KDP crystals of equal length. Data is given for fourth-harmonic generation for completeness.[10]

The angular acceptance and bandwidth are often quoted in terms of the FWHM's $\Delta\theta_{FWHM}$ and $\Delta\lambda_{FWHM}$. It is important to note that these quantities relate to the "tuning curves" obtained for monochromatic, unidirectional beams propagated at a varying wavelength or angle. The cases involving a broadband beam, or a beam containing large intrinsic divergence (a spread of angles), are more complicated as they entail nonlinear interactions between the different modes that can lead to the introduction of broadening and structure to the $k$ and $\omega$ spectra.[12]

Table 36.II
Sensitivity of conversion crystals to errors in angle and wavelength.

| | $\Delta\theta_{FWHM}$ mrad | $\Delta\lambda_{FWHM}$ Å | $\Delta\theta/\Delta\lambda$ mrad/Å | $\Delta\theta_{90}$[(c)] mrad | $\Delta\lambda_{90}$[(c)] Å |
|---|---|---|---|---|---|
| Tripler (type-II KDP)[(a)] | | | | | |
| 1 cm, small signal | 1.560 | 9.554 | −0.163 | 0.312 | 1.911 |
| 1.6 cm, small signal | 0.975 | 5.971 | −0.163 | 0.195 | 1.194 |
| 1.6 cm, high conversion[(d)(f)] | 0.488 | 2.986 | −0.163 | 0.098 | 0.597 |
| Doubler (type-II KDP)[(a)] | | | | | |
| 1 cm, small signal | 3.207 | 154.485 | −0.021 | 0.641 | 30.897 |
| 1.6 cm, small signal | 2.004 | 96.553 | −0.021 | 0.401 | 19.311 |
| 1.6 cm, high conversion[(e)(f)] | 2.004 | 96.553 | −0.021 | 0.401 | 19.311 |
| Quadrupler (type-I KDP)[(b)] | | | | | |
| 1 cm, small signal | 1.985 | 1.363 | −1.453 | 0.397 | 0.273 |

Notes:

(a) Optimum operating intensities for tripling are 4 GW/cm$^2$ (1-cm doubler and tripler) and 1.5 GW/cm$^2$ (1.6-cm doubler and tripler).

(b) Frequency quadrupling would probably be done with thickness 0.5–1.0 cm depending on two-photon absorption constraint.

(c) $\Delta\theta_{90}$ = shift from peak, which gives 90% of peak conversion. Table uses $\Delta\theta_{90} = 0.2\ \Delta\theta_{FWHM}$; similarly for $\Delta\lambda$.

(d) Use half the small-signal values; this applies when approximately 80% overall conversion is achieved.

(e) Use small-signal values for sensitivity of overall tripling to doubler errors. This is an attractive feature of the polarization-mismatch scheme.[11]

(f) Values quoted are not greatly different between single rays and averages over a temporal Gaussian.

(g) All angles are measured in air.

E4811

The quantities $\Delta\theta_{FWHM}$ and $d\lambda_{FWHM}$ are inversely proportional to the crystal thickness. The ratio $\Delta\theta/\Delta\lambda = n\ d\theta_m/d\lambda$, where $n$ is the refractive index of KDP, is proportional to the rate of change of phase-matching angle $\theta_m$ with respect to $\lambda$, and is independent of crystal thickness or operating intensity.

Suppose that the crystals are tuned to the phase-matching angle corresponding to a given wavelength. The quantities $\Delta\theta_{90}$ and $\Delta\lambda_{90}$ are the shifts in angle (exterior to the crystal) and wavelength that reduce the conversion efficiency to 90% of its peak value. To a good

approximation, they are a factor of 5 smaller than the FWHM's. Near the peak of the tuning curve the relationship is close to quadratic: e.g., shifts of $\Delta\theta_{90}/3$ or $\Delta\lambda_{90}/3$ would reduce the efficiency by 1%. These values would be important for the reproducibility of a system with, say, a requirement of 1% beam balance. For tripling with our current 1.6-cm crystals, $\Delta\theta_{90}$ = 98 $\mu$rad and $\Delta\lambda_{90}$ = 0.597 Å.

Correction of the phase-matching angle for a beam whose wavelength $\lambda_0$ shifts linearly in one direction across the cross section is easily performed using a pair of weak cylindrical lenses, as shown in Fig. 36.16. These lenses could be used as windows for the conversion cell. At each point $y$ in the beam the spectrum has a peak $\lambda_0$ ($y$), which is a linear function of $y$, and a width $\delta\lambda$, which is independent of $y$. For example, for a spatial dispersion factor ($y_{max}/D$) of 10, a variation of $\lambda_0$ by $d\lambda_{max}$ = 10 Å across the beam implies $\delta\lambda$ = 1 Å, so that locally the spectrum is $\lambda_0(y)\pm 0.5$ Å. The local spectral width is (just) within the $\Delta\lambda_{90}$ of our current system, and so we would expect minimal degradation of conversion, although the actual degradation (resulting from the nonlinear mode-mode interactions mentioned above) could be greater. This degradation would be uniform across the beam aperture. In spite of this uncertainty, 1 Å seems a reasonable value to require for $\delta\lambda$. From Table 36.II, the half-angle $\Psi$ of decollimation = 0.163 ($d\lambda_{max}/2$) = 0.815 mrad.

The doubler tuning is unaffected by this decollimation, since the sensitive direction of the doubler is orthogonal to that of the tripler. (If instead we were to use a spherical decollimation, rays at the edges of the doubler would be mismatched by 0.815 mrad, about 2 $\Delta\lambda_{90}$, leading to non-negligible losses in these regions.) The wavelength error incident on the doubler, $\pm 5$ Å in our example, is well within $\Delta\lambda_{90}$ = 19 Å, so the doubling efficiency is not compromised. The doubler bandwidth does, however, limit the maximum feasible $d\lambda_{max}$, with 10% at the edge of the beam (2.5% overall) lost when $d\lambda_{max}$ = 40 Å. Larger bandwidths than this would not propagate satisfactorily (i.e., with uniform amplification in the frequency domain) through the system due to the finite gain bandwidth of Nd:glass.

The wavelength acceptance of KDP for fourth-harmonic generation is several times smaller; one would then need a much larger spatial dispersion factor to achieve the same $d\lambda_{max}$.

**Propagation Issues**

Some issues associated with the successful propagation of a spectrally dispersed beam are discussed in this section.

1. Diffraction

Figure 36.15 shows how the shape of the beam cross section changes from point $A$ (input to gratings $G_1$ and $G_2$), to point $B$ (output from gratings), and to point $C$ (after reshaping to a circular cross section). At $A$, all frequency components in the original beam overlap spatially and are assumed to have a flat phase front. Each component propagates along a different path through the gratings (and through or

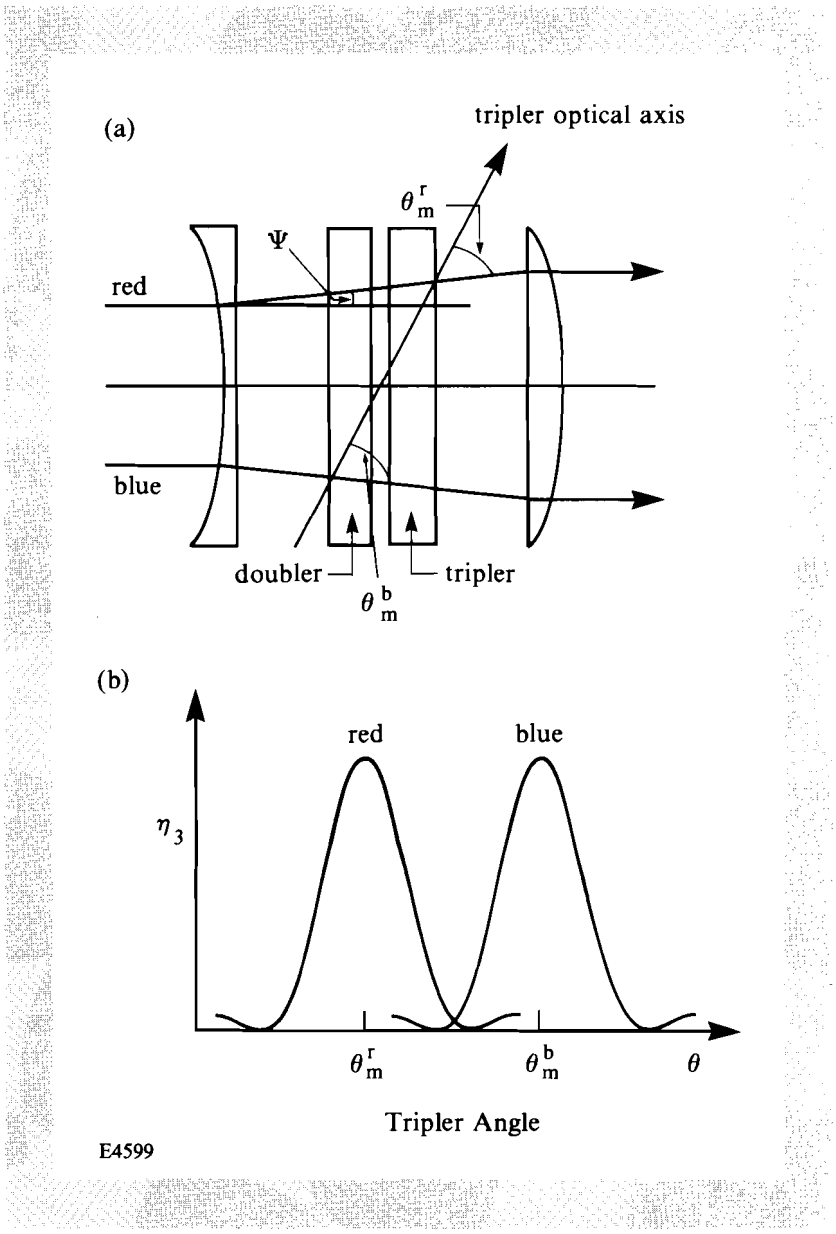


Fig. 36.16
Correction of phase-matching angle for a beam whose spectrum varies linearly across the beam aperture: (a) the imposition of a cylindrical divergence causes the red and blue portions of the spectrum to make different angles with the tripler optic axis; (b) overall third-harmonic conversion efficiency, $\eta_3$ as a function of the angle between the beam and the tripler optic axis. The optimum angle $\theta_m$ varies linearly with frequency.

reflected off an echelon or another diffractive element, not shown or specified here, to compensate for the time delay of the red component), maintaining its circular shape and size if diffraction spreading is small. After beam reshaping (point *C*) the resultant beam is approximately square, but could be apodized to circular if desired.

Each frequency component occupies an elliptical cross section, with width reduced by the spatial dispersion factor. This reduced width will result in increased diffraction spreading as this component propagates through the system. For this reason the limit of complete spatial dispersion ($\delta\lambda \rightarrow 0$), which has some interesting and unusual features, is unattainable. Whether diffraction is a problem for the spatial dispersion factors of order 10 under consideration remains to be determined.

2. Divergence

If diffraction can be neglected, good propagation through the system requires that each frequency component have a flat phase front across the beam aperture. This is especially important because the beam reshaping will cause phase errors to occur across a smaller transverse distance; equivalently, the intrinsic divergence in the direction of spectral dispersion is increased by the spatial dispersion factor. This is a concern for frequency conversion, which is sensitive to divergence: from Table 36.II, $\Delta\theta_{90} = 100$ $\mu$rad for our current crystals at high conversion.

3. Source of Broad-Bandwidth Input

The physical means by which the broad bandwidth is produced are important. Consider first a frequency-chirped pulse, such as is produced by an optical fiber where, approximately, the frequency increases linearly during the pulse, and assume that the relative path-length delay through the gratings has been corrected. On examination of the beam shape at point *C* in Fig. 36.15, the energy in the beam would be delivered in an elliptical subaperture that would move across the beam in time. This would be unacceptable for two reasons: (a) instantaneous intensities would be increased by the spatial dispersion factor (say 10), and (b) the focusing lens would see only one frequency at each time, thereby voiding the desired interference between frequencies. There is a related problem: if for some reason the input pulse were produced without the broad bandwidth, it would propagate through the system with ten times the desired intensity. It is therefore highly desirable that the frequency spectrum of the input be uniform throughout the pulse, and spread uniformly between $\lambda_0 \pm d\lambda/2$, in order to avoid operating with an unacceptably low fill factor.

One theoretical possibility might be to spectrally disperse a longer pulse (say 10 ns) through a fiber, so that each frequency component would have the desired duration ($\sim$1 ns), and then impose large relative delays ($\sim$10 ns or 3 m) on the red portion of the spectrum to bring the components together in time. This seems to be impractical, not least because Raman scattering prevents the use of fibers in this regime.

Another possibility might be to propagate a discrete number of different frequencies, each assigned to a discrete portion of the beam. In order to obtain good on-target smoothing, a large number ($\gtrsim$ 50 ?) of such frequencies would be needed, since otherwise time-independent phase relationships would be maintained over large spatial regions of the focusing lens.

4. Interference Effects

Interference effects in the laser between overlapping spectral components have not yet been considered. The simple model we have implicitly assumed, whereby individual Fourier components propagate independently until they add in the target plane to give the target irradiation pattern, is valid for propagation through linear elements in the laser chain but may not provide a correct treatment of nonlinear processes such as self-focusing and frequency conversion.

**Calculations of Beam Smoothing**

Consider a beam propagating in the $z$-direction that passes through a random phase mask (RPM) with square elements of diameter $d$ and is focused at a distance $F$ from the mask. For simplicity assume the beam has a constant near-field amplitude. Then the electric field $E$ in the target (focal) plane is given by[13]

$$E(x,y) \sim \operatorname{sinc}\left(\frac{xd}{\lambda F}\right) \operatorname{sinc}\left(\frac{yd}{\lambda F}\right) \times Re\sum_{k,\ell} \exp\left[-\frac{2\pi}{\lambda F} i(X_k x + Y_\ell y) + i\phi_{k\ell} + i\tilde{\phi}_{k\ell}(t)\right], \quad (4)$$

where $(k, \ell)$ refer to an individual element of the RPM, $(X_k, Y_\ell)$ is the center of the element measured from the beam axis, and $\phi_{k\ell}$ is the static phase imposed on the beam. The spatially dispersed spectrum introduces an additional phase variation across the beam, which is assumed to be of the form

$$\tilde{\phi}_{k\ell}(t) = \omega_0 t + \Delta\omega \frac{R+Y_\ell}{2R} t \quad ,$$

where $R$ is the radius of the near-field beam, and $\Delta\omega$ is the spread in frequency. It should be noted that this is a highly simplified model, since it neglects the overlap at each point on the near field of a range of Fourier components.

The intensity $I$ will vary as $|E|^2$. Separating out the phase terms and neglecting terms that vary as $2\omega_0 t$, we have

$$I(x,y,t) = I_0(x,y) x \sum_{\substack{k,\ell \\ m,n}}^{N} \cos\left\{-\frac{2\pi}{\lambda F}[(X_k - X_m)x + (Y_\ell - Y_n)y] + (\phi_{k\ell} - \phi_{mn}) + \frac{\Delta\omega t}{2R}(Y_\ell - Y_n)\right\}, \quad (5)$$

where $N$ is the number of phase plate cells in one direction. The target will respond to the time-average intensity, averaged over the characteristic hydrodynamic time scale. The average is

$$\bar{I}(x,y,t) = \frac{1}{t}\int_0^t I(x,y,t')\,dt'$$

$$= N^2 I_0(x,y) + I_0 \sum_{\substack{k\neq m \\ \ell}} \cos\left[\frac{-2\pi}{\lambda F}(X_k - X_m)\,x + (\phi_{k\ell} - \phi_{m\ell})\right]$$

$$+ \frac{1}{\Delta\omega t} I_0 \sum_{\substack{\ell\neq n \\ k\neq m}} \left[\frac{2R}{Y_\ell - Y_n} \sin\left[-\frac{2\pi}{\lambda F}(X_k - X_m)\,x + (\phi_{k\ell} - \phi_{mn})\right.\right.$$

$$\left. + \left(\frac{\Delta\omega t}{2R} - \frac{2\pi}{\lambda F} y\right)(Y_\ell - Y_n)\right]$$

$$\left. - \frac{2R}{Y_\ell - Y_n} \sin\left\{-\frac{2\pi}{\lambda F}\left[(X_k - X_m)\,x + (Y_\ell - Y_n)y\right] + (\phi_{k\ell} - \phi_{mn})\right\}\right]. \quad (6)$$

Part of the interference term is seen to decrease as $1/\Delta\omega t$. Further, the effect of time averaging is found to be similar to the effect of a one-dimensional spatial average in the direction of wavelength dispersion. Temporal smoothing is most rapid for interference between beams produced the furthest apart ($Y_\ell - Y_n$ the largest), which produces the short-wavelength structure. The long wavelength is reduced on a longer time scale. This is illustrated in Figs. 36.17–36.20, which show horizontal and vertical cuts through the far-field (target-plane) beam for $\Delta\omega t/2\pi = 1$, 10, 25, and $\infty$, respectively. For the example of a 10-Å bandwidth in the IR, the first three correspond to averaging times approximately of 1, 10, and 25 ps.

There will always be a residual interference variation along the direction perpendicular to the wavelength dispersion, as seen in Fig. 36.20 ($t = \infty$) and Eq. (6). The oscillations around the smooth envelope have peak-to-valley variations of about $1/\sqrt{N}$). The example in Fig. 36.20 uses a 100 × 100 phase plate, and the resultant peak-to-valley oscillations are ±5%.

## ACKNOWLEDGMENT

This work was supported by the U. S. Department of Energy Office of Inertial Fusion under agreement No. DE-FC08-85DP40200 and by the Laser Fusion Feasibility Project at the Laboratory for Laser Energetics, which has the following sponsors: Empire State Electric Energy Research Corporation, New York State Energy Research and Development Authority, Ontario Hydro, and the University of Rochester. Such support does not imply endorsement of the content by any of the above parties.

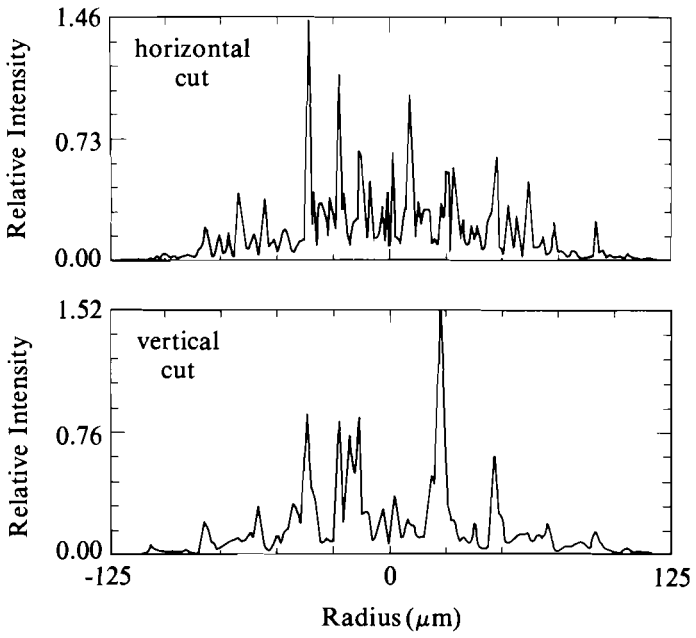


Fig. 36.17
Calculation of the effect of smoothing by spectral dispersion showing horizontal and vertical cuts through the far-field beam for $\Delta\omega t/2\pi = 1$.

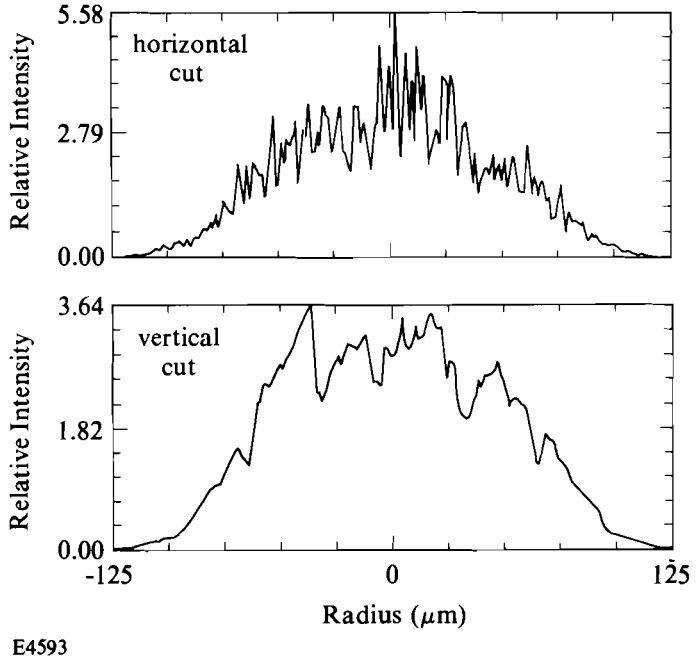


Fig. 36.18
Same as Fig. 36.17 with $\Delta\omega t/2\pi = 10$.

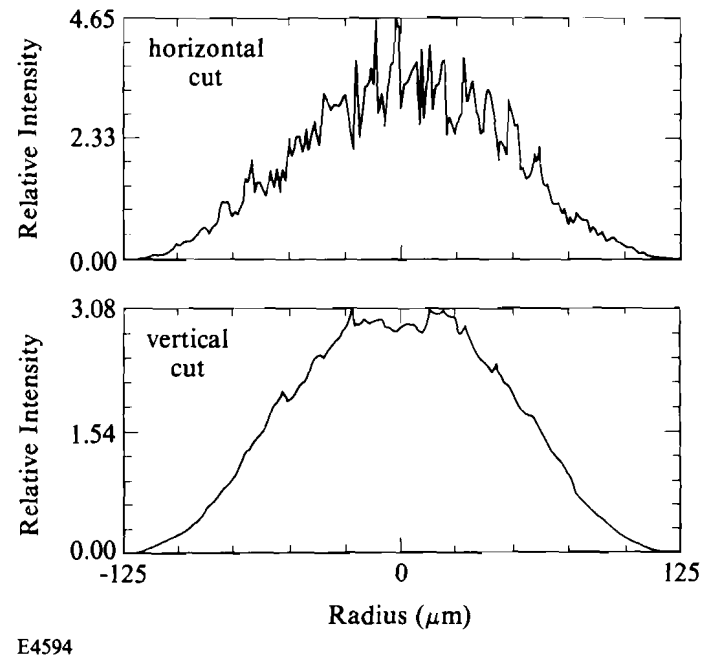


Fig. 36.19
Same as Fig. 36.17 with $\Delta\omega t/2\pi = 25$.

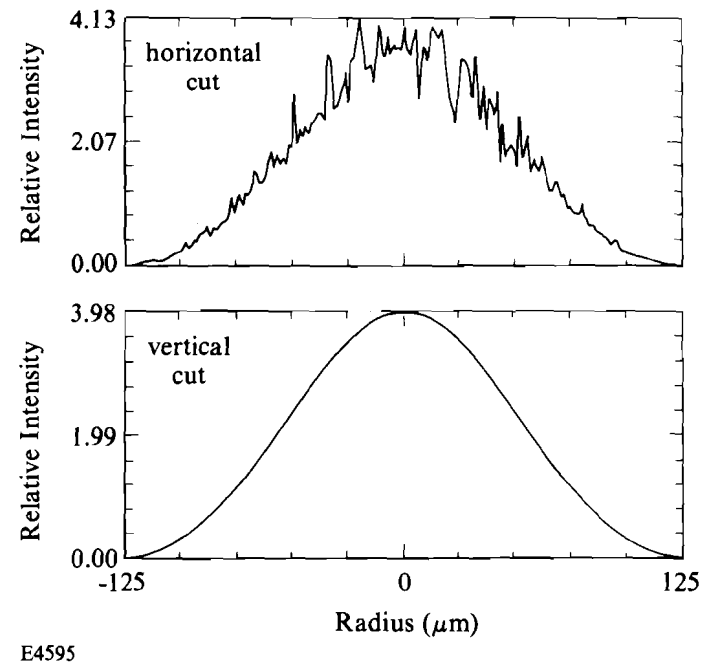


Fig. 36.20
Same as Fig. 36.17 with $\Delta\omega t/2\pi = \infty$.